

Reflection Loss from a “Pierson–Moskowitz” Sea Surface Using the Nonlocal Small Slope Approximation

Shira L. Broschat

Abstract— The lowest-order nonlocal small slope approximation (NLSSA) reflection coefficient is derived, and numerical results are presented for one-dimensional (1-D) surfaces, satisfying the Dirichlet boundary condition. Reduction to the perturbation expression occurs in the small height limit, and the first term of the reflection coefficient gives the Kirchhoff approximation (KA) result. Numerical results for the reflection loss at low grazing angles using a Pierson–Moskowitz spectrum are compared with those of other approximate methods as well as with exact integral equation (IE) results. For those cases when exact results are available, the NLSSA is found to give accurate results, comparable to those of the small slope approximation (SSA) and superior to those of classical perturbation theory (PT) and the KA.

Index Terms— Acoustic scattering, electromagnetic reflection, electromagnetic scattering by rough surfaces, radar scattering, remote sensing, sea surface electromagnetic scattering.

I. INTRODUCTION

Numerical results for the incoherent bistatic scattering strength for the nonlocal small slope approximation (NLSSA) for scattering from rough surfaces [1], using a Gaussian spectrum, were recently reported [2]. The cases considered agreed with exact integral equation (IE) results and demonstrated the potential of the NLSSA for accurate modeling of rough surface scattering. In this paper, results for the coherent reflection loss for one-dimensional (1-D) surfaces are presented. The lowest-order NLSSA reflection coefficient is derived, and numerical results for the reflection loss are obtained for low grazing angles for acoustic scattering from pressure-release surfaces or TE-polarized electromagnetic scattering from perfectly conducting surfaces. To enable comparison with exact numerical results, calculations are limited to 1-D surfaces with Gaussian statistics, satisfying a Pierson–Moskowitz power law spectrum. However, the results for two-dimensional (2-D) surfaces should be consistent with those for 1-D surfaces. Numerical results are compared with perturbation theory (PT), Kirchhoff approximation (KA), small slope approximation (SSA), and IE results. Both the NLSSA and SSA results agree with the IE results and are superior to those of PT and the KA. A number of cases are presented for which exact results are unavailable. For these cases, it is found that the NLSSA and SSA results diverge as the frequency is increased.

II. NLSSA

The NLSSA was introduced by Voronovich as a generalization of the SSA [1], [3], [4] that would explicitly include nonlocal interactions. Toward this end, Voronovich iterated the second-kind IE, retaining the double scattering term. Then, as with the SSA, a systematic series related to generalized surface slopes was formulated. It was shown that, in the high frequency limit, the NLSSA generally accounts for double scattering and, in the appropriate conditions, the lowest-order NLSSA reduces to the second-order SSA, where second order refers to the field, not to the intensity.

Manuscript received January 14, 1998; revised March 27, 1998. This work was supported by the Office of Naval Research, Code 3210A.

The author is with the School of Electrical Engineering and Computer Science, Washington State University, Pullman, WA 99164-2752 USA (e-mail: shira@eecs.wsu.edu).

Publisher Item Identifier S 0196-2892(99)00125-4.

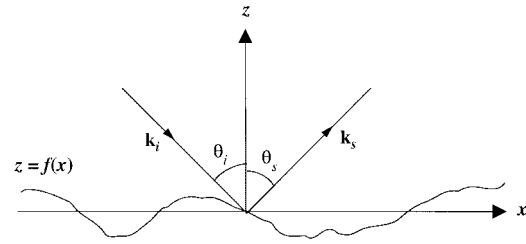


Fig. 1. Scattering geometry.

A. Lowest-Order NLSSA T -Matrix

The NLSSA T -matrix for 1-D surfaces $z = f(x)$, satisfying the Dirichlet boundary condition, is given by

$$T(k_{sx}, k_{ix}) = -\frac{2\kappa_{iz}}{v_z} \frac{1}{(2\pi)^2} \int dx_1 \int dx_2 \int dK_1 \cdot \exp[-i(k_{sx} - K_1)x_1 - ik_{sz}f(x_1)] \cdot \exp[i(k_{ix} - K_1)x_2 - ik_{iz}f(x_2)] \cdot \Phi(k_{sx}, k_{ix}; (x_1 + x_2)/2, K_1, [F]) \quad (1)$$

where the limits of integration here and elsewhere are infinite, $\vec{k}_i = (k_{ix}, k_{iz}) = (k_{ix}, -\kappa_{iz}) = k(\sin \theta_i, -\cos \theta_i)$ is the incident wave vector, $\vec{k}_s = (k_{sx}, k_{sz}) = k(\sin \theta_s, \cos \theta_s)$ is the scattered wave vector, k is the wavenumber, $v_z = \kappa_{iz} + k_{sz}$, and $\vec{r}_1 = (x_1, f(x_1))$ and $\vec{r}_2 = (x_2, f(x_2))$ are points on the surface. The scattering geometry is shown in Fig. 1. In (1), Φ represents the unknown surface field and is independent of both vertical and horizontal translations of the surface, and a harmonic time dependence of $e^{-i\omega t}$ is assumed. The $[F]$ argument of Φ represents the dependence of Φ on $F(K)$, the Fourier transform of $f(x)$. Φ is expanded in a functional Taylor series of $F(K)$ to give

$$\Phi = \Phi_0(k_{sx}, k_{ix}; K_1) + \int dK_2 \exp[iK_2(x_1 + x_2)/2] \cdot \Phi_1(k_{sx}, k_{ix}; K_1, K_2)F(K_2) + \int dK_2 \int dK_3 \exp[i(K_2 + K_3)(x_1 + x_2)/2] \cdot \Phi_2(k_{sx}, k_{ix}; K_1, K_2, K_3)F(K_2)F(K_3) + \dots \quad (2)$$

The Φ_n 's are found by comparison with the PT T -matrix in the small height limit. For the lowest-order NLSSA, only the Φ_0 term is retained. Comparison with PT gives

$$\Phi_0 = 1 + \left(\frac{k\beta_1}{\kappa_{iz}} - 1 \right) + \left(\frac{k\beta_1}{k_{sz}} - 1 \right) \quad (3)$$

where

$$k\beta_1 = \sqrt{k^2 - K_1^2}. \quad (4)$$

In (4), the square root is taken to be positive for $k^2 > K_1^2$ and positive imaginary for $k^2 < K_1^2$. The lowest-order NLSSA T -matrix T_0 is obtained from (1) and (3)

$$T_0(k_{sx}, k_{ix}) = -\frac{2\kappa_{iz}}{v_z} \frac{1}{(2\pi)^2} \int dx_1 \int dx_2 \int dK_1 \cdot \exp[-i(k_{sx} - K_1)x_1 - ik_{sz}f(x_1)] \cdot \exp[i(k_{ix} - K_1)x_2 - ik_{iz}f(x_2)] \cdot \left[1 + \left(\frac{k\beta_1}{\kappa_{iz}} - 1 \right) + \left(\frac{k\beta_1}{k_{sz}} - 1 \right) \right] \quad (5)$$

where $k\beta_1$ is given by (4).

B. Lowest-Order NLSSA Reflection Coefficient

The scattered field ψ_s is given in terms of the T -matrix by

$$\psi_s(\vec{r}) = \int dk_{sx} \exp[ik_{sx}x + ik_{sz}z]T(k_{sx}, k_{ix}) \quad (6)$$

and the reflection coefficient is thus given by

$$\begin{aligned} \langle R \rangle &= \frac{\langle \psi_s \rangle}{\psi_i} \\ &= e^{-ik_{ix}x + ik_{iz}z} \int dk_{sx} \exp[ik_{sx}x + ik_{sz}z] \langle T(k_{sx}, k_{ix}) \rangle \end{aligned} \quad (7)$$

where the angle brackets indicate an ensemble average and ψ_i is the plane-wave incident field. Calculation of the ensemble average yields a Dirac delta function with argument $k_{sx} - k_{ix}$. Thus, as expected, coherent reflection occurs only in the specular direction. For the lowest-order NLSSA, (5) is used to approximate $T(k_{sx}, k_{ix})$ in (7). The ensemble average of T_0 is of the form $\langle e^{i\alpha_1 X_1} e^{i\alpha_2 X_2} \rangle$, where X_1 and X_2 are zero-mean Gaussian random variables. This expression is evaluated as $\exp[-(\alpha_1^2 + \alpha_2^2)\sigma^2/2 - \alpha_1\alpha_2 K_{12}]$ where σ^2 is the variance and $K_{12} = \langle X_1 X_2 \rangle$ [5]. After converting to sum and difference coordinates, the lowest-order NLSSA reflection coefficient is obtained

$$\langle R \rangle_{NLSSA} = -e^{-2\chi^2} - \frac{1}{\pi\kappa_{iz}} e^{-2\chi^2} I \quad (8)$$

$$I = \int dK_1 \sqrt{k^2 - K_1^2} g(K_1) \quad (9)$$

$$g(K_1) = \int dx e^{i(K_1 - k_{ix})x} [e^{-\chi^2[C(x)-1]} - 1] \quad (10)$$

where $C(x)$ is the surface correlation function, $\chi = \kappa_{iz}h$, and h is the rms surface height. The first term of (8) is the KA reflection coefficient, and in the small height limit, (8) with (9) and (10) reduces to the second-order (in the field) perturbation result.

C. Approximation of the Lowest-Order NLSSA Reflection Coefficient

The double integral given by (9) with (10) is nontrivial to calculate. In addition to the oscillatory nature of the integrand, the order of integration must be preserved—that is, the x integration of (10) must precede the K_1 integration of (9). If the order is reversed, divergence occurs. When $k^2 > K_1^2$, I is purely real; when $k^2 < K_1^2$, I is purely imaginary. Calculating the real part of I poses no difficulty; however, calculating the imaginary part is difficult if not impossible. In Fig. 2, the integrand functions of (9) are plotted as a function of K_1 for one of the cases considered in the next section. The solid line shows the function $g(K_1)$ [the integral given by (10)], and the dashed line (beta) shows the square root function. At the branch points—that is, when $K_1 = \pm k$ —the square root function changes from real to imaginary and grows in value approximately linearly for $|K_1| > k$. On the other hand, $g(K_1)$ has a sharp peak at $K_1 = k_{ix}$ and is oscillatory elsewhere with the amplitude of the oscillations decreasing in size approximately linearly with increasing $|K_1|$ and the frequency of the oscillations increasing with increasing $|K_1|$. The combined behavior of the square root function and $g(K_1)$ for increasing $|K_1|$ is the reason why I is difficult to evaluate numerically.

Numerical calculation of the NLSSA reflection coefficient given by (8) with (9) and (10) is not very practical, and it is even less practical for 2-D surfaces. However, Fig. 2 suggests an approximation that might give good results while reducing the complexity of the calculation substantially; the major contribution to the integral I occurs in the vicinity of the peak in $g(K_1)$ at $K_1 = k_{ix}$. At normal incidence, the peak occurs at $K_1 = 0$; at 90° incidence,

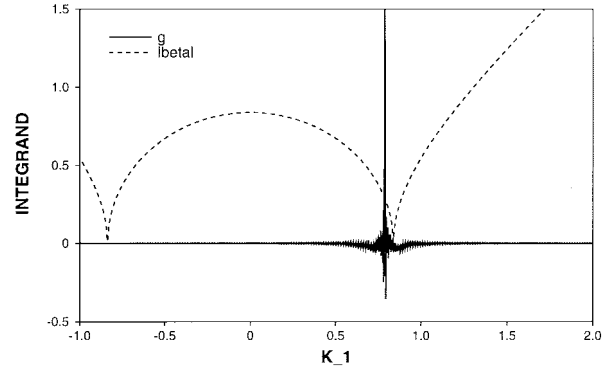


Fig. 2. Integrand functions of (9) for an angle of incidence of 70° , a wind speed of 10 m/s, and $kh = 0.45$. $g(K_1)$ (solid line) is the x integral given by (10), and $|\beta(K_1)|$ (dashed line) is the magnitude of the square root function of (9). Branch points occur at $K_1 = k$; β is real for $|K_1| < k$ and imaginary for $|K_1| > k$.

it occurs at $K_1 = k_{ix}$; and at all other angles of incidence, it falls between zero and k_{ix} . Thus, most of the contribution to the reflection coefficient comes from the real part of I , particularly for small angles of incidence. At larger angles of incidence, the imaginary part of I may make an appreciable contribution (although at 90° , the square root function vanishes and the reflection coefficient is zero). However, as shown in the next section, even for an incident angle of 80° , the real part of I can give excellent results. If we truncate the imaginary part of I —that is, if we integrate only between the two branch points occurring at $\pm k$ when I is purely real—the integrals of (9) and (10) can be interchanged and the dK_1 integral becomes a Bessel function. The approximate form of the lowest-order NLSSA reflection coefficient is then given by

$$\langle R \rangle_{NLSSA} \cong -e^{-2\chi^2} - \frac{2k}{\kappa_{iz}} e^{-2\chi^2} I \quad (11)$$

$$I = \int_0^\infty dx \cos(k_{ix}x) \frac{J_1(kx)}{x} [e^{-\chi^2[C(x)-1]} - 1] \quad (12)$$

where $J_1(kx)$ is the Bessel function of the first kind of order one. Thus, elimination of the imaginary part of the reflection coefficient reduces the double integral to a single integral, a considerable simplification, and as shown below, the results are excellent.

III. NUMERICAL RESULTS

In this section, we present results for the approximate form of the lowest-order NLSSA reflection coefficient given by (11) and (12) for a Pierson–Moskowitz spectrum [6]. The results are limited to large angles of incidence for which it is generally more difficult to obtain accurate results. The NLSSA results are compared with those of PT, the KA, the SSA, and an “exact” Monte Carlo IE technique. (By exact, we mean that no approximations are made to the underlying physics of the IE and the solution can be obtained to the degree of accuracy required by the problem.) The Pierson–Moskowitz frequency spectrum is an approximate model of the ocean surface, which is completely determined by the wind speed. It represents a fully developed sea state with multiscale roughness. The spatial roughness spectrum for a 1-D surface is obtained from the frequency spectrum [7]

$$W(K) = \frac{\alpha}{4|K|^3} \exp\left[-\frac{\beta g^2}{K^2 u^4}\right] \quad (13)$$

where α and β are dimensionless constants given by 8.1×10^{-3} and 0.74, respectively, $g = 9.81 \text{ m/s}^2$ is the earth’s acceleration due to

TABLE I
COHERENT REFLECTION LOSS IN DECIBELS USING THE NONLOCAL SMALL SLOPE APPROXIMATION RL_{NLSSA} , THE INTEGRAL EQUATION METHOD RL_{IE} , THE SMALL SLOPE APPROXIMATION RL_{SSA} , PERTURBATION THEORY RL_{PT} , AND THE KIRCHHOFF APPROXIMATION RL_{KA}

u [m/s]	θ_i [deg]	kh	RL_{NLSSA}	RL_{IE}	RL_{SSA}	RL_{PT}	RL_{KA}
10	70	0.45	0.360	0.359	0.358	0.366	0.406
20	80	1.79	1.551	1.519	1.519	1.644	1.676
20	75	1.79	3.23	3.24	3.27	4.07	3.72
20	70	1.79	6.01	6.01	6.04	10.25	6.50

TABLE II
COHERENT REFLECTION LOSS IN DECIBELS USING THE NONLOCAL SLOPE APPROXIMATION RL_{NLSSA} , THE SMALL SLOPE APPROXIMATION RL_{SSA} , AND THE KIRCHHOFF APPROXIMATION RL_{KA} FOR $\theta_i = 80^\circ$ AND $u = 15$ m/s

f_{acous}/f_{EM} [Hz]/[MHz]	kh	RL_{NLSSA}	RL_{SSA}	RL_{KA}
100/20	0.50	0.196	0.193	0.132
200/40	1.01	0.601	0.588	0.529
300/60	1.51	1.166	1.138	1.191
400/80	2.01	1.902	1.873	2.117
500/100	2.51	2.854	2.852	3.308
1000/200	5.03	11.600	11.978	13.231
2000/400	10.05	52.390	50.930	52.923
3000/600	15.08	107.786	116.698	119.076
4000/800	20.10	138.852	209.055	211.691
5000/1000	25.13	186.626	327.939	330.767

gravity, and u is the wind speed measured at 19.5 m above the mean sea surface. The NLSSA reflection coefficient is a function of the surface correlation function $C(x)$, which is the Fourier transform of the spectrum given by (13). Calculation of the correlation function was performed as described in [7, Appendix A] using the Numerical Algorithms Group (NAG) quadrature routine d01akf, and fortieth-order Chebyshev polynomials were used to approximate $C(x)$ in (12). The same NAG routine was also used to calculate (12).

Numerical results have been obtained for a number of different cases. However, only results for the first four cases can be compared with exact results available in the literature. The first case is for an incident angle of 70° at a wind speed of $u = 10$ m/s (19 knots). The normalized roughness parameter kh , where k is the radiation wavenumber and h is the rms surface height, for this case is 0.45. The second, third, and fourth cases are for incident angles of 80° , 75° , and 70° , respectively, at a wind speed of $u = 20$ m/s (39 knots), and $kh = 1.79$. These kh and u correspond to an acoustic frequency of 200 Hz and an electromagnetic frequency of 40 MHz.

Results for the reflection loss $[20 \cdot \log\langle R \rangle]$ are given in Table I for the four cases described above. We have also tabulated the results published in [7] for the IE method, second-order (in the field) PT, and the KA and the results published in [8] for the second-order (in the field) SSA. For a description of the IE method and discussion of the statistical uncertainty of the IE results, refer to [7]. The expressions used to calculate the PT, KA, and SSA results are given in [8]. Both the NLSSA and SSA results agree with the exact numerical results given by the IE method and are superior to the PT and KA results for all four cases considered. For $\theta_i = 80^\circ$, the NLSSA and IE results differ the most; this may be due to the elimination of the imaginary part of the reflection coefficient. However, the difference is quite small, only about 2%.

IV. SUMMARY AND DISCUSSION

In this paper, we have derived the lowest-order NLSSA reflection coefficient and approximated it by its real part. This approximation

reduces the reflection coefficient from a double to a single integral that is readily calculated. Numerical results for the approximate form of the reflection loss have been compared with exact numerical results for a Pierson–Moskowitz surface spectrum at low grazing incident angles for several different cases. The results are accurate and consistently better than both the second-order perturbation and KA results.

Since the SSA reflection loss results for the cases considered are accurate, we expect the NLSSA results to be as well. The accuracy of the approximate expression for the NLSSA reflection coefficient was not guaranteed, however, and is thus a pleasant discovery. Results presented in [2] for the incoherent scattering cross section for a Gaussian spectrum showed that, for $kh = 9$, the NLSSA is more accurate than the second-order SSA at low forward grazing angles. Also, at an acoustic frequency of 5 kHz or an electromagnetic frequency of 1 GHz for $u = 10$ m/s ($kh = 11.17$) and $\theta_i = 70^\circ$, the behavior of the integrand of (9) is similar to that of the integrand shown in Fig. 2. Therefore, there is some indication that the approximate NLSSA reflection coefficient should give accurate results at higher frequencies when the SSA will not. In Table II, we present results for the NLSSA, SSA, and KA for a fixed wind speed $u = 15$ m/s, a fixed incident angle $\theta_i = 80^\circ$, and increasing frequencies. The rms surface height h is completely specified by the wind speed and is 1.2 m, peak to trough. The frequencies range between 100 Hz and 5 kHz for acoustics and 20 MHz and 1 GHz for electromagnetics. From Table II, we see that, as the frequency is increased, the NLSSA and SSA results differ significantly. It remains to be seen which of these, if any, is accurate.

ACKNOWLEDGMENT

The author wishes to thank J. Schneider for helpful suggestions and E. Thorsos for helpful discussions.

REFERENCES

- [1] A. G. Voronovich, "Nonlocal small-slope approximation for wave scattering from rough surfaces," *Waves Random Media*, vol. 6, pp. 151–167, 1996.
- [2] S. L. Broschat and E. I. Thorsos, "A preliminary numerical study of the nonlocal small slope approximation," *J. Acoust. Soc. Amer.*, vol. 100, p. 2702, 1996.
- [3] A. G. Voronovich, "Small-slope approximation in wave scattering by rough surfaces," *Sov. Phys. JETP*, vol. 62, pp. 65–70, 1985.
- [4] E. I. Thorsos and S. L. Broschat, "An investigation of the small slope approximation for scattering from rough surfaces. Part I. Theory," *J. Acoust. Soc. Amer.*, vol. 97, pp. 2082–2093, 1995.
- [5] S. L. Broschat and E. I. Thorsos, "An investigation of the small slope approximation for scattering from rough surfaces. Part II. Numerical studies," *J. Acoust. Soc. Amer.*, vol. 101, pp. 2615–2625, 1997.
- [6] W. J. Pierson, Jr., and L. Moskowitz, "A proposed spectral form for fully developed wind seas based on the similarity theory of S. A. Kitaigorodskii," *J. Geophys. Res.*, vol. 69, pp. 5181–5190, 1964.
- [7] E. I. Thorsos, "Acoustic scattering from a 'Pierson–Moskowitz' sea surface," *J. Acoust. Soc. Amer.*, vol. 88, pp. 335–349, 1990.
- [8] S. L. Broschat, "The small slope approximation reflection coefficient for scattering from a 'Pierson–Moskowitz' sea surface," *IEEE Trans. Geosci. Remote Sensing*, vol. 31, pp. 1112–1114, Nov. 1993.